PAPER • OPEN ACCESS

Predicting the geological condition beyond the tunnel excavation face using MSP monitoring data and LSTM algorithm

To cite this article: Je-Kyum Lee and Sean Seungwon Lee 2023 *IOP Conf. Ser.: Earth Environ. Sci.* **1124** 012007

IOP Conf. Series: Earth and Environmental Science 1124 (2023) 012007 doi:10.1088/1755-1315/1124/1/012007

Predicting the geological condition beyond the tunnel excavation face using MSP monitoring data and LSTM algorithm

Je-Kyum Lee, Sean Seungwon Lee

Department of Earth Resources and Environmental Engineering, Hanyang University, Seoul 04763, Korea; leejk1991@hanyang.ac.kr

seanlee@hanyang.ac.kr

Abstract. The ground conditions beyond an excavation face, especially discontinuities in rock masses, have a significant influence on tunnel construction. However, the actual ground conditions observed during tunnel construction are often different from the ground conditions predicted in the geotechnical site explorations carried out in the design stage. Changes in ground conditions may require alterations in tunnel design, leading to substantial disruptions in the construction schedule and budget. In this regard, accurate ground evaluation prior to the design and construction stages are essential for successful tunnel construction projects. Machine learning models have been developed in order to evaluate the condition of rock discontinuities within 50 m of the tunnel face. Machine data (rotational pressure, feed pressure, and drilling (advance) speed) obtained from a large boring hole machine, called MSP, at an NATM construction site in a granite formation located in South Korea were logged, and the actual ground Discontinuity Score (DS) was appraised by analysing internal bore hole images taken after drilling. Then, the LSTM algorithm was applied to develop the machine learning model to determine DS based on the logged machine data. DS was most accurately predicted when the drilling speed was included in the input data, whereas those cases using only the rotational and feed pressure in the input data showed low prediction accuracy. Therefore, the drilling speed seems to have a higher correlation than hydraulic pressure with regard to ground conditions, including discontinuities. Once additional data is collected from various tunnel sites, the machine learning model could be further enhanced to become more robust and provide solutions to various engineering problems.

1. Introduction

Accurate evaluation of ground conditions is essential in tunnel construction because it influences the tunnel design, construction schedule, and budget. Despite numerous geotechnical explorations, including boring, seismic, and resistivity surveys, unfamiliar ground conditions are often encountered during construction, resulting in modifications to the original design, additional costs, and delays in the construction schedule; thereby, it introduces the need for skilled engineers who can precisely determine ground conditions, all of which makes tunnel construction an arduous task.

Therefore, various attempts have been made to assess ground conditions at a low cost. Several studies have been conducted using convolutional neural networks (CNNs), which show decent performance in image recognition among machine learning techniques, to evaluate the rock grade of a tunnel face [1, 2, 3]. In addition, a machine learning model for recognising joint traces from images of rock has been

IOP Conf. Series: Earth and Environmental Science 1124 (2023) 012007 doi:10.1088/1755-1315/1124/1/012007

developed through a combination of machine learning algorithms such as gradient boosting tree (GBT), random forest (RF), decision tree (DT), and multi-layer perceptron (MLP) [4].

The methods mentioned above are limited in that the evaluation is only possible for the excavated area. Thus, several studies are being performed in order to pre-emptively determine the rock quality beyond the excavation face. Using a drilling machine like the jumbo drill, which is used for tunnel construction, makes it possible to predict the ground condition beyond the tunnel face during construction. Attempts to use drilling machines to predict ground conditions have been conducted gradually since 1968, at which the relationship between uniaxial compressive strength (UCS) and drilling speed was investigated [5]. Since then, relationships between drilling vibration, rock texture, and strength have also been determined [6]. Recently, cases of research using machine learning algorithms have increased. In 2008, an artificial neural network (ANN) was used with Tunnel Seismic Prediction (TSP) exploration data to predict the rock mass rating (RMR) in front of the tunnel face [7]. Properties of rock such as UCS, density, tensile strength, mineral composition, and RMR are derived from the drilling data (bit diameter, penetration rate, sound level, etc.) by ANN, Gaussian Process (GP), support vector machine (SVM), and RF [8, 9, 10, 11].

The data acquired from the drilling machines correspond to ground conditions 2-5 m beyond the tunnel face, or one or two construction cycles, resulting in unexpected additional time to handle unfamiliar ground conditions. Instead, using the data of the large hole boring machine called MSP, ground conditions corresponding to the drilling length, about 50-60 m ahead of tunnel face, can be assessed. Therefore, this study proposes a method to predict the rock conditions from MSP data using the long short-term memory (LSTM) algorithm, which is advantageous in time series data analysis.

2. Methodology

Recurrent neural network (RNN) algorithms have been used widely to analyse sequential data such as time series data because they use a hidden state which contains output values of the hidden layer in the previous input data (Figure 1a). However, the RNN has a drawback where the gradient could vanish as the length of the input sequence increases. As a result, the algorithm cannot manage long-range dependency.

Hochreiter and Schmidhuber developed the LSTM algorithm in 1997 to deal with the vanishing gradient problem of RNNs [12]. LSTM uses the h-vector and cell state vector (Figure 1b). The h-vector contains information about previous cells, whereas the cell state vector contains long-term information. When an input value is fed, the cell state vector is updated, selectively accepting the information from the previous cell state vector (forget gate) and current input values (input gate). After that, the output values of the hidden layer (h_t) are calculated using the new cell state vector and the previous output values (h_{t-1}) (output gate). With a series of these operations, LSTM can build a model that can handle both short-term and long-term information.

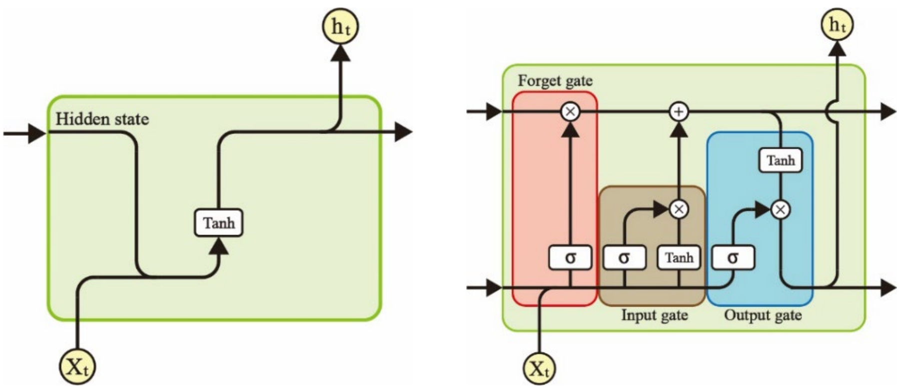

(a) RNN algorithm (b) LSTM algorithm

Figure 1. The structure of each algorithm.

3. Data collection

3.1. Site description
The monitoring data was collected from an NATM water tunnel that directly connects a river to the East Sea, in order to control the flow rate of the rivers located in Ganggu-myeon, Yeongdeok-gun, Gyeongsangbuk-do, South Korea (Figure 2). The tunnel width is 5.4 m, the height is 4.6 m, and the length is 746 m. The site is composed of granite. The data collected cover a 100 m length of the tunnel, from No. 14.08 to No. 19.08 (Figure 3), where the overall rock quality is decent, and joints exist at some points, making it easy to distinguish the joints from bedrock.

Figure 2. Location of the tunnel.

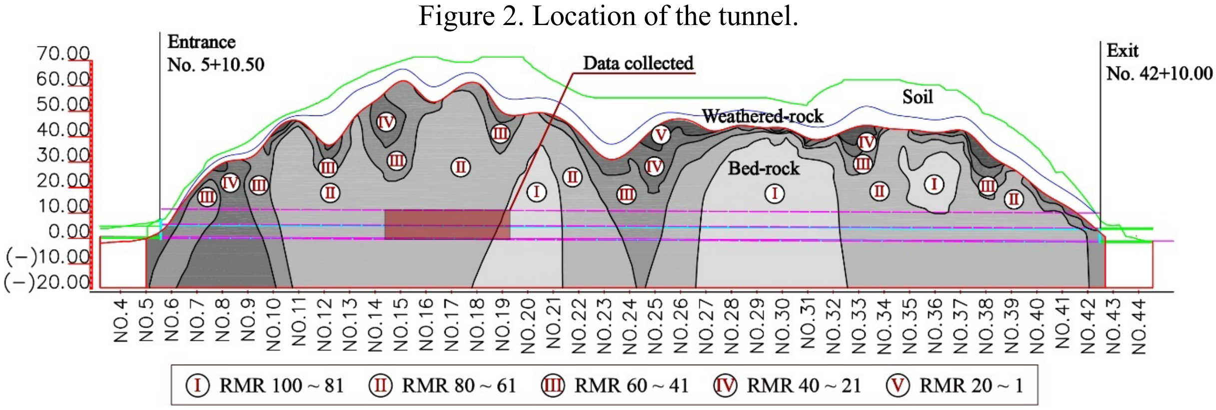

Figure 3. Longitudinal view of the tunnel.

3.2. Machine data
MSP was used to drill a large-diameter hole at the centre of the tunnel face, adding a free surface to the tunnel face and reducing blast vibrations. It is similar to the parallel cut method, but the most distinctive feature is the drilling size, usually about 350 to 400 mm in diameter and about 50 to 60 m in length. The diameter of the hole created by the MSP is 3 to 4 times the diameter of that of the parallel cut, decreasing the blast vibrations and increasing the blast efficiency.

The drilling operation is performed by three main movements: rotation, feed, and percussion. Hydraulic pressure is used for the rotation and feed, and air pressure for the percussion. Since the volume of air changes easily, it is difficult to capture the reaction of the ground to air pressure. Therefore, only two of the three main movements were monitored by recording rotational and feed pressure from the MSP machine. The drilling speed was also measured, which makes a total of three factors selected as machine data (Table 1).

Table 1. Machine data measured from the MSP.

Parameter	Description	Source	Purpose
P_r	Rotational pressure	MSP machine	Input data
P_f	Feed pressure	MSP machine	Input data
V_d	Drilling speed	MSP machine	Input data

3.3. *Discontinuity Score (DS)*

Discontinuities, such as joints and faults, are the primary causes of shear failure and act as paths of groundwater inflow. For this reason, discontinuities have been regarded as a key factor in major rock mass classification systems (RMR, Q, GSI, etc.). A probing device was used to obtain information related to discontinuities and the internal images of the drilled hole were captured. Based on the captured images, we are proposing a new indicator, namely Discontinuity Score (DS). It was created and used to evaluate the intensity of the discontinuities. DS criteria are shown in Figure 4. If there is one or less discontinuity in 1 m of drilling, DS is 1 (Figure 4a). If two to four discontinuities exist in 1 m, DS is 2 (Figure 4b). A DS of 3 indicates that there are more than five discontinuities crossing each other in 1 m (Figure 4c). If the discontinuities are more intense than that, DS is evaluated as 4. This includes cases where partial collapse occurs only with a small excavation with a 380 mm drill diameter, or the severe trace of water flow like rust is observed (Figure 4d).

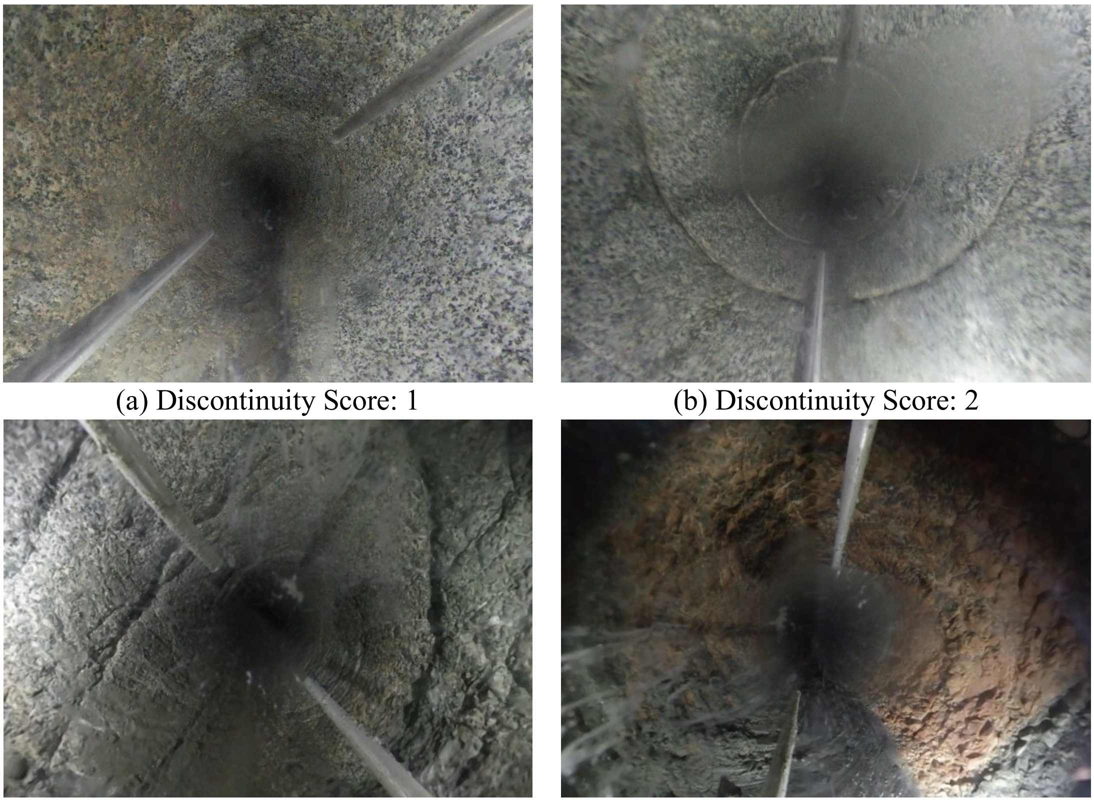

(c) Discontinuity Score: 3 (d) Discontinuity Score: 4

Figure 4. Example images corresponding to Discontinuity Score (DS) of 1 to 4.

3.4. Pre-processing

The collected data needs to be modified appropriately for the analysis. First, machine data related to extra-drilling work, such as preparation before drilling, rod extension, or rod removal was removed to leave drilling-related data only. Second, the DS was multiplied by four to emphasise the scores' contrast. Third, the drilling speed was calculated using wire sensor data that recorded the accumulated moving distance. Finally, a total of 100 m of data was divided into two parts; the first half was used for testing, and the second half was used for training. Figure 5 shows the pre-processed data.

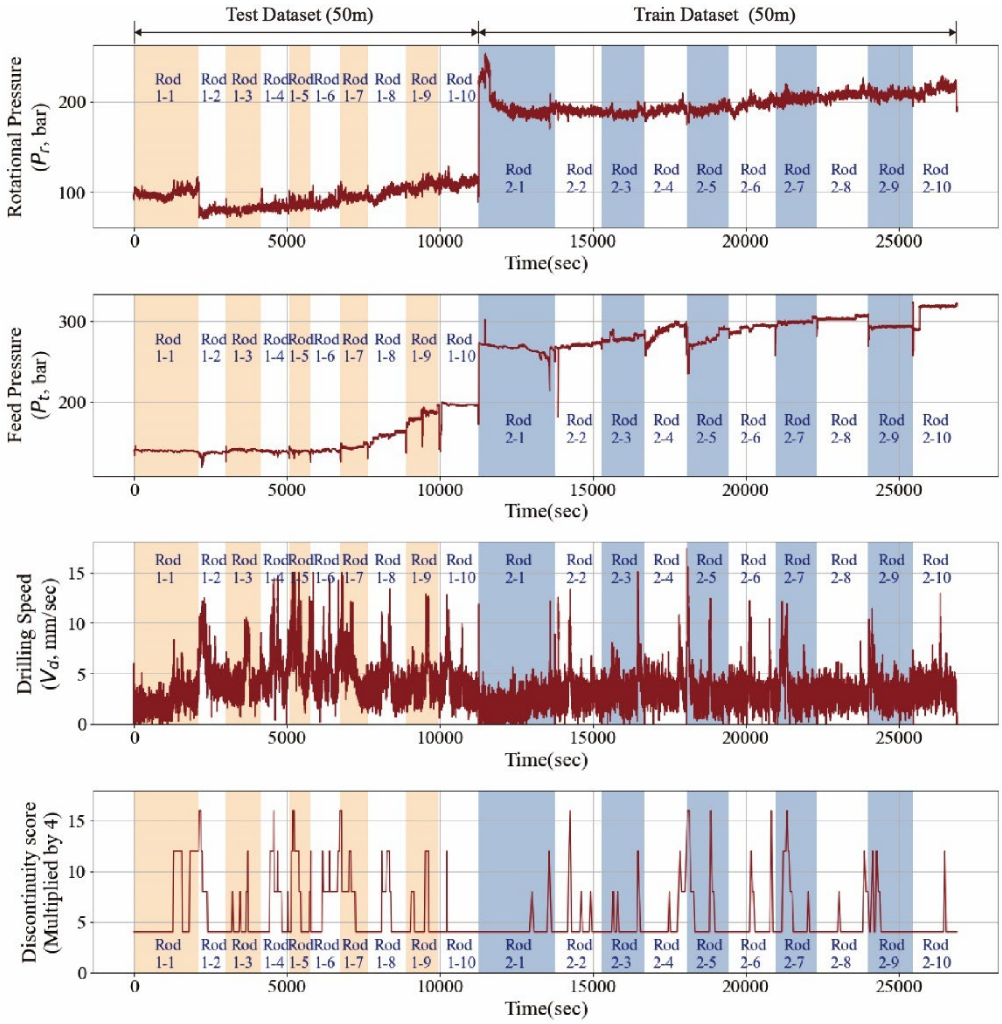

Figure 5. Pre-processed MSP data.

4. Machine learning result and discussion

The structure of the prediction model is shown in Figure 6. There are three LSTM layers and three fully connected layers (FCL) connected to each other. The number of nodes starts at 150 in the first LSTM layer and continuously decreases through each layer in the order of 70, 32, 32, 16, 1. Sigmoid, Relu, and Linear functions were used as the activation function in the FCL. Epoch was set to 100, batch size was set to 50, and mean squared error (MSE) was used as the loss function. Nine cases of input data were used applying various combinations of machine data, as shown in Table 2, to account for the various relationships between the machine data and DS.

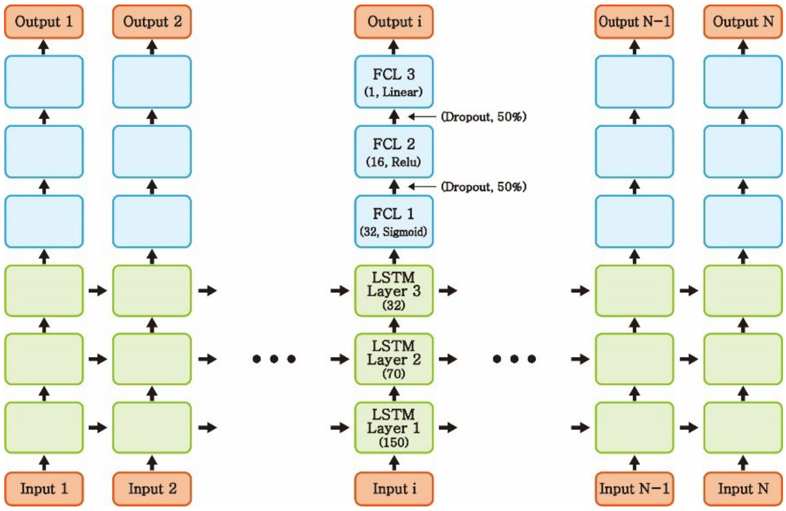

Figure 6. Model Structure.

Table 2 Input cases and loss value.

Case number	Case 1	Case 2	Case 3	Case 4	Case 5	Case 6	Case 7	Case 8	Case 9
Inputs	P_r	P_f	V_d	$P_r \times P_f$	$P_r \times V_d$	$P_f \times V_d$	$P_r \times P_f \times V_d$	V_d/P_r	V_d/P_f
Train loss	5.656	5.670	2.591	5.601	2.071	2.609	2.464	2.153	3.147
Test loss	10.644	10.482	8.320	10.606	7.751	8.227	7.911	7.780	8.514
Remark		-			(Element wise product)			(Element wise division)	

The general performance of the LSTM model was assessed by the mean value of the test losses generated from ten models for each input case. The average test loss at the end of the epoch can be seen in Table 2, where Case 5 shows the best performance with a test loss of 7.751. Figure 7 shows the average test loss according to epochs for Case 5. As the epoch increases, the test loss steadily decreases and maintains a constant value after epoch 35, whereas train loss keeps decreasing, which indicates that the models are slightly over-fitted. Other than Case 5, the test cases with test losses lower than nine were, from lowest to highest, Cases 8, 7, 6, 3, and 9. The remaining three cases showed test losses higher than ten. The consistent factor across these three cases was that the drilling speed was not used as an input. This indicates that the drilling speed is a key factor in the prediction algorithm.

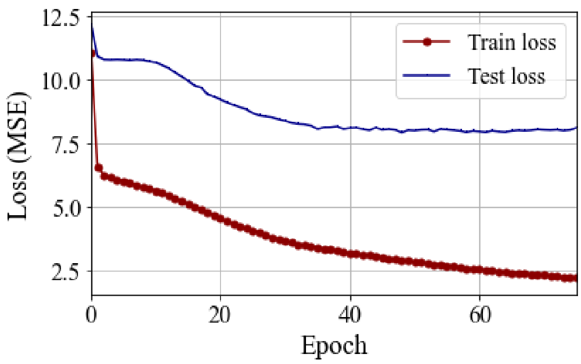

Figure 7. Averaged loss (MSE) of test data (Input Case 5).

The performance of Case 5 can be reviewed in detail by comparing the predicted DS of the models with the actual DS for the training and testing data. Figure 8 shows the actual and predicted DS using the training data. The predicted DS was smaller to the actual score, but the locations of the predicted region where the DS is 3 or higher were relatively consistent with the actual region. Figure 9 shows the actual and predicted DS using the test data. The predicted scores were not as accurate as the scores that were used in the training data. However similar trends were observed, which shows a difference in the size of the DS and the regional accuracy high enough to specify the areas where DS is 3 or more.

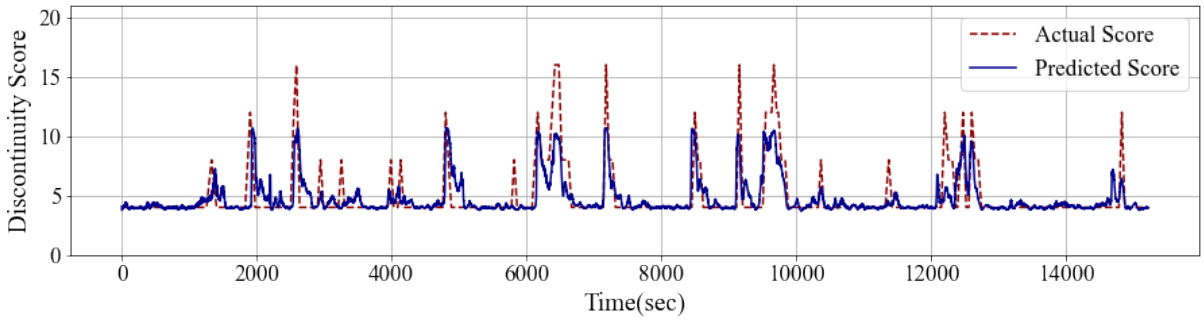

Figure 8. Predicted result of training data (Input Case 5).

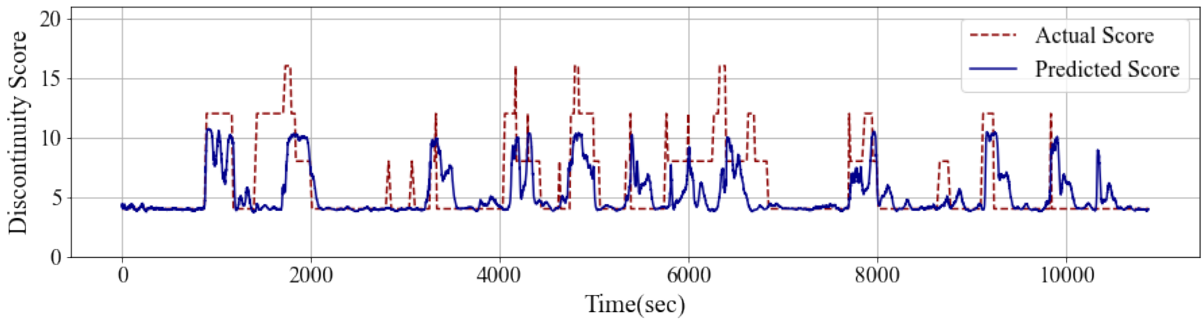

Figure 9. Predicted result of testing data (Input Case 5).

5. Conclusion

In this study, discontinuities beyond the tunnel face were predicted using the LSTM algorithm and MSP data. The MSP machine data was collected from the NATM site and a new indicator, namely Discontinuity Score (DS), was created and used to evaluate the intensity of the discontinuities. The machine learning structure was composed of six layers; three LSTM layers and three FCLs, and nine input cases were applied according to various combinations of the machine data. As a result, Input Case 5, in which Element-wise product of P_r and V_d is used as input, showed the best DS prediction performance with a test error of 7.751.

The predicted DS was smaller than the actual score, but the prediction was accurate enough to specify the location of the discontinuous region where DS was 3 or higher. Therefore, the overall prediction result seemed to be sufficiently acceptable to be applied on-site because the critical factor for the structural stability is the several-metre-long joints, rather than the centimetre-scale joints.

The machine learning model developed in this study can be used to predict DS 50 m in front of the tunnel face, corresponding to the drilling distance of the MSP machine. Assuming a site with an average excavation distance of 5 m per day, the ground conditions can be predicted ten days before excavation, securing enough time to prepare for unexpected ground conditions, which can minimise the budget loss and ensure safety of human life.

Large amounts of time and effort are required for the evaluation of DS from probe images, and human subjectivity cannot be completely removed. For this reason, DS can be predicted more accurately by combining an image recognition technique like CNN.

DS only considers the number of discontinuities per metre. However, by collecting additional data such as RMR and Q to reflect the other rock properties, like rock strength, discontinuity direction, or surface roughness of discontinuity, it is expected that the ground conditions in front of the tunnel face can be predicted more accurately, which can increase the tunnel safety and minimise the disruptions in the construction schedule and budget.

References

[1] Kim HY, Cho LH, Kim KS 2019 Rock Classification Prediction in Tunnel Excavation Using CNN. Journal of the Korean Geotechnical Society. 35(9): 37-45.
[2] Lee KB, Shin HS, Kim SH, Ha DM, Choi IS 2019 A Study on Automatic Classification of Characterized Ground Regions on Slopes by a Deep Learning based Image Segmentation. Tunnel and underground space. 29(6): 508-522.
[3] Pham C, Shin HS 2020 A feasibility study on application of a deep convolutional neural network for automatic rock type classification. Tunnel and underground space. 30(5): 462-472.
[4] Chen J, Huang H, Cohn GA , Zhang D, Zhou M 2021 Machine learning-based classification of rock discontinuity trace: SMOTE oversampling integrated with GBT ensemble learning. International Journal of Mining Science and Technology. Available from: https://doi.org/10.1016/j.ijmst.2021.08.004
[5] Tsoutrelis CE 1969 Determination of compressive strength of rock in situ of in test bloacks using diamond drill. International Journal of Rock Mechanics and Mining Sciences. 6(3): 311-21.
[6] Bameri A, Seifabad MC, Hoseinie SH 2021 Laboratorial studies for the prediction of rock texture and hardness using vibration measurement while drilling. Bulletin of Engineering Geology and the Environment. 80(11): 8311-8318.
[7] Alimoradi A, Moradzadeh A, Naderi R, Salehi MZ, Etemadi A 2008 Prediction of geological hazardous zones in front of a tunnel face using TSP-203 and artificial neural networks. Tunnelling and Underground Space Technology. 23(6): 711-717.
[8] Kumar BR, Vardhan H, Govindaraj M, Saraswathi PS 2013 Artificial neural network model for prediction of rock properties from sound level produced during drilling. Geomechanics and Geoengineering. 8(1): 53-61.
[9] Hernández MG, Menéndez M, Fuente MJ, Sainz-Palmero GI 2018 Monitor-While-Drilling-based estimation of rock mass rating with computational intelligence: The case of tunnel excavation front. Automation in Construction. 93: 325-338.
[10] Khushaba RN, Melkumyan A, Hill AJ 2021 A Machine Learning Approach for Material Type Logging and Chemical Assaying from Autonomous Measure-While-Drilling (MWD) Data. Mathematical Geosciences. Available from: https://doi.org/10.1007/s11004-021-09970-w
[11] LIU J, JIANG Y, SAKAGUCHI O 2021 Influence of geological conditions of rock mass ahead of tunnel face on the prediction performance of uniaxial compressive strength prediction model. IOP Conference Series: nEarth & Environmental Science; 2021. 861(4): 1-9.
[12] Hochreiter S, Schmidhuber J 1997 Long Short-Term Memory. Neural Computation. 9(8): 1735-1780.